Near Net Shape Forming of Magnesium Alloys Superplastically – Computational Analysis and Experimental Investigations

J Kandasamy[1], Anjaiah Madarapu[2], D Sri Sai Ganesh[1]

[1]Department of Mechanical Engineering, MVSREC, Nadergul, Hyderabad – 501 510, INDIA
[2]Department of Mechanical Engineering, GNI, Ibrahimpatnam, Hyderabad – 501 506, INDIA

Abstract

Superplasticity is the ability of a polycrystalline material to exhibit in a generally isotropic manner, a very high tensile elongation prior to failure. A 3D finite element axisymmetric analysis of Magnesium alloys, AZ31B is performed in square shape dies with inserts for height variation in the MARC software. The SuperPlastic Forming (SPF) process was simulated using a viscoplastic model of the Backofen's equation. Near net shape forming of square shaped components with different L/D ratios are manufactured in the indigenously built SPF assembly set up. The FEA generated pressure time diagram is given as input to the experimental investigations. The thickness distributions of the FEA results closely correlate with the formed components. Minimum thinning in less SPF time of near net shape formed components could be achieved.

Keywords: Near Net Shape Forming, Superplasticity, Finite Element Analysis, MARC, Square components, Forming Depth, Validation

1. INTRODUCTION

"Superplasticity is the ability of a polycrystalline material to exhibit in a generally isotropic manner, very high tensile elongation prior to failure" [1]. SPF is a sheet metal forming process used to deform such materials under controlled conditions of temperature and strain rate. SPF has become a viable process in manufacturing of aircraft and automotive parts. In superplastic forming process, the uniformity of sheet thickness during and after forming is vital for ensuring the mechanical quality of the formed component. The SPF technique seems to go hand-in-hand with magnesium alloys due to the vast usage as structural parts in automotive sector. Magnesium alloys components produced through SPF posseses improved anti-fatigue, anti-corrosion properties of the structure with light weight and high strength.[1−6]. The superplastically formed part exhibits non-uniform thickness distribution because of stretch forming nature of the process.[7,8] This leads to the increase of weight and reduction of the integral property of the parts, and easily causes cracks and decreases the forming limit of materials.[9] Therefore, the non-uniform thinning limits the practical application of superplastic forming. The direct-reverse superplastic forming process an effective approach to improve the thickness uniformity, consists of two stages: firstly, the sheet was formed into the pre-forming die to pre-thin material in local regions, and then the pre-formed sheet was blow formed into the forming die to obtain the final shape.[10] A simple form of constitutive equation for superplastic material is given by Backofen $\boldsymbol{\sigma=K\dot{\varepsilon}^m}$ [3] where σ flow stress, K strength coefficient, $\dot{\varepsilon}$ strain rate, and m strain rate sensitivity index. Three mechanisms namely vacancy creep, creep by grain boundary diffusion, and grain boundary sliding accounts for the high strain-rate sensitivity found in superplastic materials. The strain-rate sensitivity of metals arises from the viscous nature of the deformation process.[11 – 15] Mathematical modeling of the superplastic forming operation at a constant strain rate condition, developed in two simple equations relates required gas pressure to the material parameters. It predicts the thickness variation between the pole and the equator. Simulation results of SPF in conical die by 2D model with axisymmetric elements and 3D model with shell elements in ABACUS are observed to be similar [8]. Titanium alloys superplastic deformation capability is demonstrated by successful forming Ti-Al-Mn alloy into hemispherical components.[9] The influence of friction depends on the type of bulging on the die geometry. This is analyzed by FE technique and validated experimentally on conical bulging and rectangle box bulging.[17] Investigations on a series of axisymmetric models on the influence of component shape and the contact friction on the final thickness distribution reveals a small friction coefficient can improve the uniformity of the thickness. For a rectangular box bulging, as friction decreases, the filling ability of the sheet towards the die corner and the uniformity of the thickness increases.[16-17] The literature available indicates that the research was performed on the development of SPF for various alloys. However, any breakthrough in the processing of sheet materials is more likely to come from the development of new alloys with very high formability at low temperature and various strain rates. The development of superplastic forming technique is to improve formability of existing alloys that will relax the precise requirements. The thickness distribution, effective stress, effective strain, critical damage characteristics of the formed sheet depends on the material properties K and m. The forming time in superplastic forming is a function of die entry radius, die angle, die diameter, height of the die and friction coefficient between the sheet and die. The optimum pressure-time diagram, controls the pressure to maintain the target strain rate and minimizes the thinning and forming time. The hot deformation behavior of AZ series magnesium alloys is due to large manganese intermetallic particles. Cavitation and diffuse necking is the main cause for failure, the mechanism being the difference in distribution of particles. Several authors have reported the change in philosophy, today's choices and developments in the SPF process, its cost effectiveness, SPF major role in producing airframes, engine structures. Superplastic forming of components with abrupt change in shapes leading to near net shape forming is very scantily available in the literature. [18 – 26] Research in the recent past related to superplastic forming is widely attempted experimentally and numerically on regular shapes, but only few researchers have performed superplastic forming analysis on

ISBN: 978-93-80689-28-9

forming depth of practical components in automotive and aerospace industries in rectangle shaped dies. [27 – 34] The paper presents the computational simulations of superplastic forming in magnesium alloy AZ31B sheets. The forming profiles of a regular rectangular die with different depth of forming is computationally analyzed. The results of the Finite Element (FE) model is successfully demonstrated to predict the forming behavior and verified experimentally for thickness of forming.

2. MATERIALS AND METHODS

The magnesium alloy, AZ31B, has various industrial applications because of its special characteristics such as light weight, high stiffness. A sheet of Mg alloy of 1 mm thickness is used in this study. The constitutive model proposed as power law by Backofen. et al. is the widely applied model that relates the effective strain, strain rate, stress and flow stress through power law. The chemical composition and the mechanical properties of the alloy Magnesium AZ31B is shown in Table.1 and 2 respectively. The alloy is characterized for a temperature range of 450^0C and a strain rate of 0.001 s^{-1}. The material property values are experimentally found to be K = 254 MPa (Constant), strain rate sensitivity index m = 0.518, strain hardening index n = 0.87.

Table 1. Chemical Composition of AZ31B

Alloy	Al	Zn	Mn	Si	Cu	Ni	Mg
% by weight	2.9	1.1	0.49	1.0	0.1	0.03	Balance

Table.2 Mechanical Properties of AZ31B

Property	Yield Strength	Ultimate Strength	Melting Point	Modulus of Elasticity	Poisson ratio
Value	220 MPa	290 MPa	630^0 C	45 GPa	0.35

3. COMPUTATIONAL ANALYSIS

Numerical simulations are performed in MSC.MARC, implicit nonlinear finite element analysis software, used to simulate the superplastic forming behavior of materials under large strains. Computational analysis for magnesium alloy sheets of 1 mm thickness is formed superplastically in a rectangular die with different depth of forming as 60mm, 40 m and 20 mm. The model of the die and the simulation of the process are shown in Fig.1. The model is meshed with 3D 400 Quad (4) elements. The sheet is defined as deformable body (visco-elastic) and the die is defined as rigid plastic body. The contact bodies are assigned with coulomb friction for interaction during forming and with a friction coefficient (μ) of 0.3 between sheet and die. Boundary conditions involve fixing the edges of the sheet in all degrees of freedom and the remaining sheet is left unconstrained. The gas pressure is applied on the top face of thesheet. The sheet is deformed superplastically into the rigid die by suitable pressure. The plastic behavior of the sheet during forming is controlled by the flow stress which is a function of the strain rate. During superplastic forming, the loading scheme keeps on adjusting the applied pressure to maintain an average target strain rate in the material. The optimum Pressure Time (P-T) diagram for different profiles is simulated for the better load case time. The optimum P-T diagram provides the pressure with less thickness variation between pole and equator along arc length on the formed components. As the sheet contacts the die, friction causes the thickness of the sheet to vary with time. The pressure is so adjusted to keep this strain rate sensitive material within a certain target range. This is necessary to maintain the proper flow of the superplastic material. Prediction of thinning of the sheet is another important aspect since the sheet may become too thin for its application or get punctured during the forming process. The SPF pressure control in the FE code is used to automatically adjust the pressure on the sheet to maintain the target strain rate. The computational analysis is performed to very near practical situations for the optimum load case time. The model of the die, forming process in MARC is shown in Fig.1. The variation of displacement thickness during sheet deformation for the optimum load case time, thickness distribution, Pressure-Time graph, Arc Length-Thickness variation and manufactured components are shown in Fig.2 for the different depth of forming in the rectangular die.

3. EXPERIMENTAL INVESTIGATIONS

The Superplastic Forming experiments have been performed in an indigenously built-in laboratory scale equipment embedded in the cylindrical split furnace connected to computer controlled system. The equipment consists in: (i) a blank-holder, (ii) a male and female die with different die cavity shapes for superplastic forming of the blank different forming conditions, (iii) a pneumatic circuit for gas supply with an argon cylinder, proportional electronic valves, steel tubes in proximity of the forming chamber and flexible polyurethane tubes in colder zones, (iv) an electric furnace with its electronic controller (v) thermocouples to monitor thermal condition on the furnace. The thickness distribution of the sheet, P_T graph, arc length Vs thickness distribution and the manufactured components are shown in Fig.3. The workpiece specimens are sheared from the same material lot. The specimen with a blank size of 160 mm diameter and 1.0 mm thickness with rolling direction perpendicular to the longitudinal axis is used for forming. The forming experiments are conducted at 400^0C. In heating stage the sheet in die setup is heated upto its $0.5T_m$ of melting temperature using electric heater. Argon gas pressure is introduced into the male die thus forming the sheet into the female die. The dynamic control of the pressure with respect to time during experimentation is the prime variable in manufacturing of components with uniform thickness. The pressure is computer controlled with time according to the better load case P-T graph obtained from the simulation results.

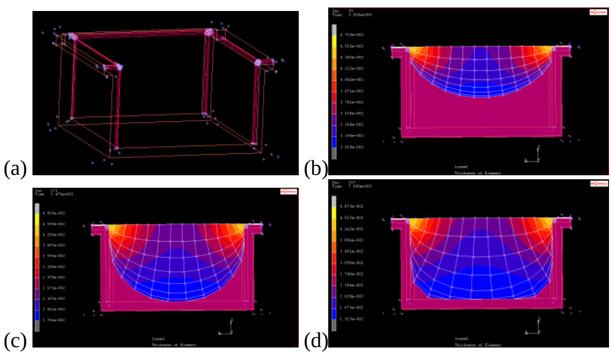

Fig. 1. (a) Square Die Model (b) Initial Stages of Free Blow Forming (c) During the start of constrained forming (d) Formed shape for optimum load case time

Forming Depth mm	Thickness Distribution	Pressure Vs Time	Arc Length Vs Thickness	Manufactured component
60	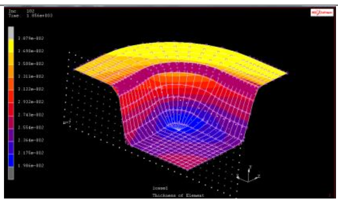	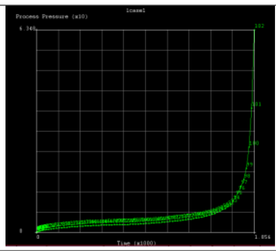	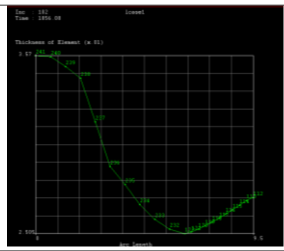	
40	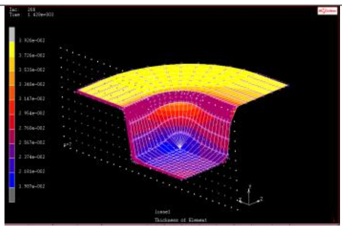	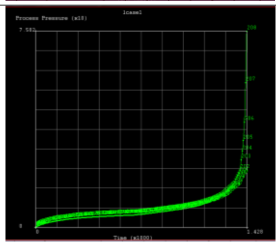	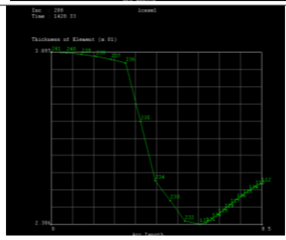	
20	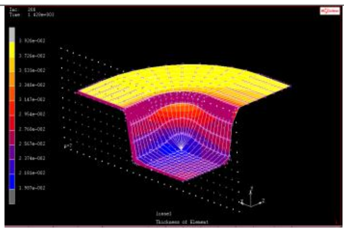	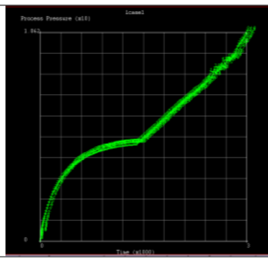	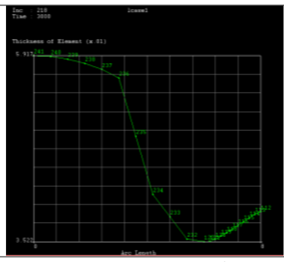	

Fig.2. (a) Thickness Distribution (b) Pressure Vs Time (c) Arc Length Vs Thickness (d) Manufactured component

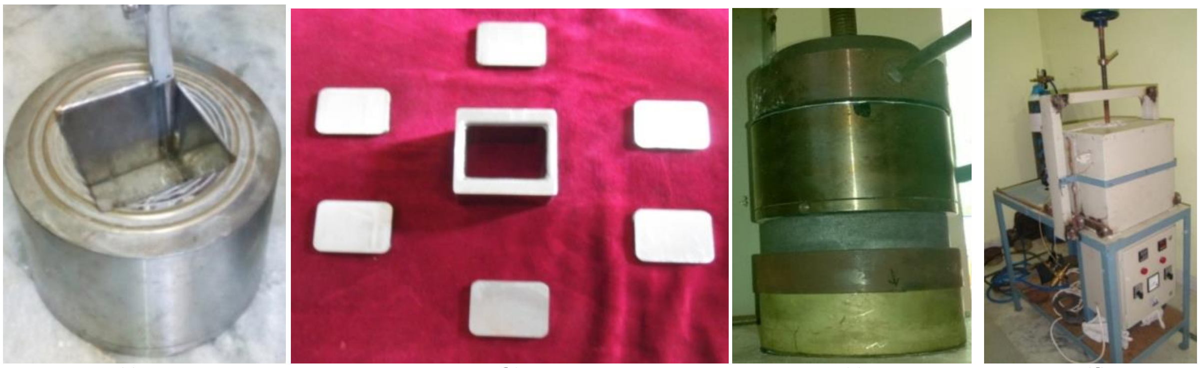

(a) (b) (c) (d)

Fig.3 (a) Square die (b) Die Inserts (c) Die assembly (d) Experimental set up

More important are the clamping loads and thermal stresses encountered during heat-up and cool-down and the environmental conditions. The thermal stresses can cause permanent distortions in the die, and this is controlled by selection of a material that has good strength and creep resistance at the forming temperature. Slow heating and cooling of the tooling can reduce the thermal stresses. Material with a low coefficient of thermal expansion and those that do not undergo a phase transformation during heating and cooling are preferred for the high temperature SPF processes. Oxidation can alter the surface condition of the tooling, thus affecting the surface quality of the SPF part produced and eventually affecting dimensional characteristics, hence argon gas is used to apply gas pressure load. To successfully form the near net shape of the component, the cavity must be sealed so that pressure applied to side of the blank is not dissipated. The seal is normally established by providing a seal bead on the tooling that engages the periphery of the sheet metal. The FE simulation results obtained from MSC Marc software are compared with the experimentation outcomes for the three different depth of forming under analysis. The results, Process Time Vs Height from pole are tabulated in Table.3 and Arc length Vs Sheet thickness in Table.4 respectively.

Table.3 Comparison of FEA with Experimentation Results for Process Time Vs Height from pole

S.No	Depth of Form, 60 mm				Depth of Form, 40 mm				Depth of Form, 20 mm			
	Process time, sec	Height from pole, mm			Process time, sec	Height from pole, mm			Process time, sec	Height from pole, mm		
		FEA	Exp	% error		FEA	Exp	% error		FEA	Exp	% error
1	2000	3	3.1	3.3	1000	24	23	3.3	1800	24	23	3.3
2	2400	6.7	6.5	2.98	2820	30	29	2.98	2000	27	26	3.7
3	3500	9.5	9.25	2.63	5470	40	38	5	4000	28	27	3.57
4	4500	13	11.7	10	7000	40	38	5	6000	30	29	3.33

Table.4 Comparison of FE with Experimentation results for Arc length Vs Sheet thickness

S.No	Depth of Form, 60 mm			Depth of Form, 40 mm			Depth of Form, 20 mm		
	Arc Length mm	Sheet Thickness mm		Arc Length mm	Sheet Thickness mm		Arc Length mm	Sheet Thickness mm	
		FEA	Exp		FEA	Exp		FEA	Exp
1	0	1	1	0	1.152	1.15	0	1	1.00
2	6.499	0.992	0.952	3.999	1.219	1.10	4.499	0.434	0.41
3	12.99	0.991	0.951	7.999	1.046	1.00	8.999	0.566	0.54
4	19.49	0.988	0.948	11.999	0.862	0.80	13.49	0.511	0.50
5	25.99	0.985	0.945	15.999	0.863	0.80	17.99	0.470	0.45
6	32.49	0.984	0.944	19.999	1.046	1.00	22.49	0.435	0.41
7	38.99	0.984	0.943	23.999	1.217	1.10	26.99	0.422	0.40
8	45.49	0.983	0.943	27.999	1.182	1.10	31.49	0.404	0.38
9	51.99	0.982	0.942	31.999	1.119	1.01	35.99	0.453	0.43
10	58.49	0.982	0.942	35.999	0.907	0.80	40.49	0.435	0.41

5. RESULTS AND DISCUSSION

The Process Time Vs Height formed and Arc length Vs Sheet thickness graphs are shown in Fig. 4 – 6 and 7 – 9 respectively. In superplastic forming using gas, the pressure is to be controlled continuously since the instantaneous magnitude influences the flow stress on the material during forming, following equilibrium mechanics. The stress induced during forming drives the material to cause the plastic deformation and subsequently the rate of strain. The pressure applied determines the time of formation. The simulated pressure time diagrams, induced better pressure control and maintained the strain rate distribution over the entire deformed surface. This has led to maximum stretching of the surface at the processed temperature. This could be substantiated by the basic theory of grain boundary sliding that takes place in fine grained superplastic materials. It is observed from Fig.4 that the superplastic forming of AZ31B depends on the gas pressure and time. For regular prismatic surfaces as shown in Fig.4, the rate of change in pressure increases gradually in a quadratic manner. This could be due to the rate of change of the thickness which is comparatively lesser than rate of change of the radius. This continues till the free bulge forming of the sheet. In this region, the rate of change of thickness increases as the radius decrease. Once the sheet contacts the die surface, the rate of change of the radius again dominates in both the stages, and an increase in pressure is observed. Similar forming behavior is observed in the 40 mm forming depth die until the die surface comes into contact. Further rapid changes in pressure with time is observed to maintain the thickness constant as shown in Fig.5 this is due to the immediate changes in the profile that requires pressure distribution differently. The die entry radius plays a major role in free forming at initial stage as more pressure is required during the initial stages of forming the component as shown in Fig.6. Higher the die entry radius lesser the pressure required at initial stage to make easy entry for sheet into die resulting in good depth. Friction between the die and sheet is related to process pressure.

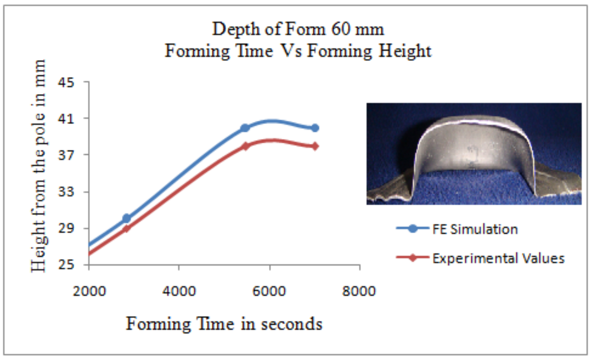

Fig.4. Forming Depth 60 mm: Forming Time Vs Depth

6. THICKNESS DISTRIBUTION

The thickness variation of the sheet decreases linearly and gradually with arc length as shown in Fig.7. This is due to free bulge forming, until the sheet touches the wall. The variation increases after the sheet makes contact with the wall. The friction coefficient between the wall and sheet resists the grain boundary sliding.

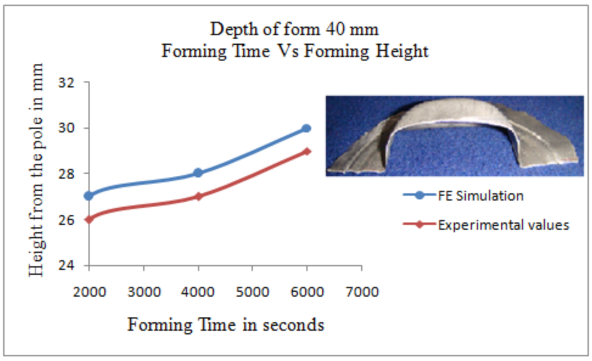

Fig.5. Forming Depth 40 mm: Forming Time Vs Depth

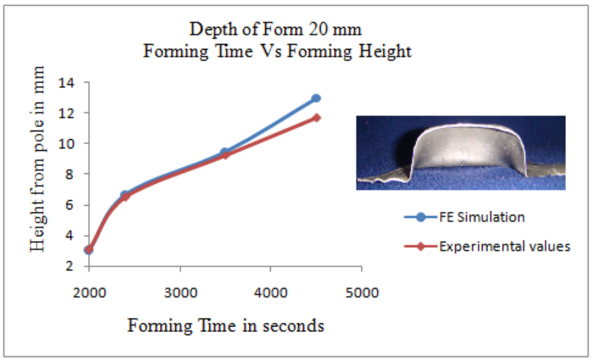

Fig.6. Forming Depth 20 mm: Forming Time Vs Depth

As the sheet makes contact with the wall surface, the thickness distribution increases to maintain constant strain-rate deformation with increase in arc length. Abrasives and lubricants are applied for optimum friction between sheets and die during formation. The thickness variation in the 40 mm depth of forming shown in Fig.8. Unevenness in thinning is observed due to material in the upper part being not stretched properly. This could be due to the portion of the material in contact with the side surfaces of the die and the grain boundary sliding reduces due to friction. The uneven thinning could be due to the aspect ratio i.e., opening width to the depth of the component being formed. The unevenness in thickness distribution may be attributed to the actual force that forms the component under plane strain conditions. The force is exerted perpendicular to the surface of the die which could be resolved into horizontal and vertical components. The horizontal component pushes the material on the die surface and the vertical component pressed down the component into the die to maintain the time and depth. The thickness variation behaves non-linearly with arc thickness due to the intricacies in the geometry of the component formed. The forming time decreases and thickness distribution values increases when the die entry radius increases. This abrupt thinning is due to the large tension exerted upon the sheet with free bulged region. As the free bulged region begins to make contact with the wall in both the steps, this rapid thinning become more profound when the die entry radius increases. The non-linear behavior of the curve shown in Fig.9 is due to sudden changes in the geometry of the specimen found.

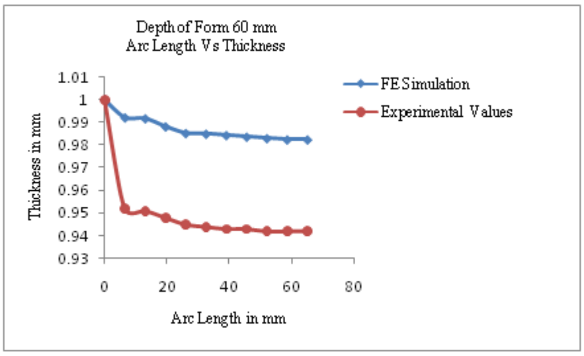

Fig.7. Forming Depth 60 mm: Arc Length Vs Thickness

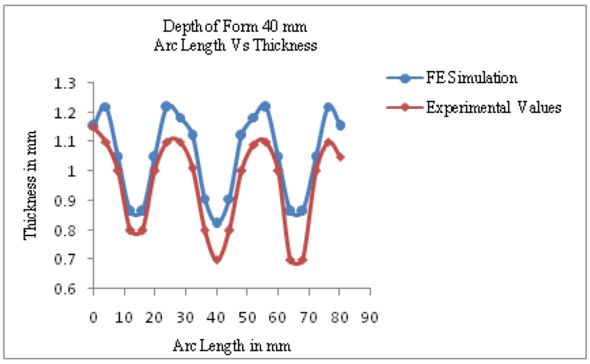

Fig.8. Forming Depth 40 mm: Arc Length Vs Thickness

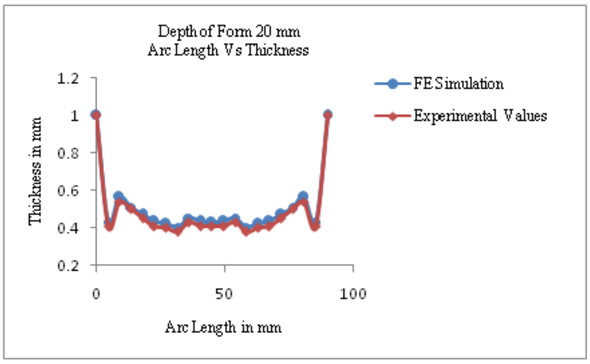

Fig.9. Forming Depth 20 mm: Arc Length Vs Thickness

7. CONCLUSIONS

Simulation results executed from the 3D FEA software MSC MARC are in good agreement with the experimental results in all the components formed with different depth investigated in this research work. It also facilitates the understanding of forming behavior of the AZ31B material by SPF.

The thickness distribution in the manufactured component is uneven in 40 m depth of form due to stick friction between the die and sheet leading to resistance in grain boundary sliding, and thus irregular stretching of the surface.

Less depth of shaped components have better strain rate, uniform stretching, less thinning with uniform thickness distribution.

ACKNOWLEDGEMENTS

The authors thank DMRL, Hyderabad for the support and guidance rendered in using MSC MARC MENTAT.

References

[1] S. Hori, M. Tokizane, “Superplasticity in Advanced Materials”, The Japan Society of Research on Superplasticity, Osaka, Japan (1991).

[2] Namas Chandra, “Constitutive Behavior of Superplastic Materials” International Journal of Non-Linear Mechanics, Vol. 37 (2002), 461-484.

[3] G.J. Davies,”Superplasticity: A Review”, Journal of Material Science, Vol. 5, (1970), 1091-1102.

[4] L.Carrino, G.Giuliano, “A posteriori optimisation of the forming pressure in superplastic forming processes by the finite element method”, Finite Elements in Analysis and Design, Vol. 39, Issue 11, (2003), 1083–1093.

[5] Abhijit Dutta, Amita K. Mukherjee, “Superplastic forming: An analytical approach” Materials Science and Engineering A, (1992), 9-13.

[6] Hambli R and Kobi S, “Optimization of superplastic forming using the finite element method” IEEE (2002).

[7] G.Y. Li, M.J. Tan K.M. Liew, “Three dimensional modeling and simulating of superplastic forming” Journal of Materials Processing Technology 150, (2004), 76-83.

[8] GAO Chong-yang and FANG You tong, “Investigation on the factors influencing the thickness distribution of superplastic formed components” Journal of Zhejiang University Science 6A (7), (2005), 711-715.

[9] Mohammad A. Nazzal et al., “Finite Element Simulation of Superplastic Forming using a Microstructure Based Constitutive Model” ABAQUS Users Conference (2005).

[10] L.Filice et al., “FE simulation and experimental considerations on Ti alloy Superplastic forming for aerospace applications”, International Journal for Material Forum, (2010), 41-46.

[11] L. M. Tang et al., “Comparative Study of Element Formulation on Simulation of Superplastic Forming”, Materials Science Forum Vols. 551-552 (2007), 281-286.

[12] Yogesha and S.S. Bhattacharya, “Superplastic forming of Ti-Al-Mn alloy”, International Symposium of Research Students on Materials Science and Engineering (2004).

[13] O.C. Zienkiewicz and R.L. Taylor, “The Finite Element Method”, Volume 1 and 2, 5th Edition, Butterworth-Heinemann, 2000.

[14] G. Kumaresan and A. Jothilingam, Experimental and FE simulation validation of sheet thickness optimization in superplastic forming of Al alloy, Journal of Mechanical Science and Technology 30 (7) (2016) 3295~3300.

[15] A. Kishchik, A. V. Mikhaylovskaya, V. S. Levchenko, V. K. Portnoy, Formation of Microstructure and the Superplasticity of Al–Mg-Based Alloys, ISSN 0031-918X, Physics of Metals and Metallography, 2017, Vol. 118, No. 1, pp. 96–103. Pleiades Publishing, Ltd., 2017.

[16] Costanzo Bellini , Gillo Giuliano, Luca Sorrentino, Free Bulging at Constant Pressure of Superplastic Sheet Metal, International Journal of Engineering and Technology (IJET), Vol. No:7, Issue No:4, August-September 2015, 1173-1178.

[17] G. Giuliano, L. Sorrentino, S. Turchetta, FEM Analysis of Superplastic PbSn60 Alloy Free Bulging Test International Journal of Engineering and Technology (IJET), Vol. N:7, issue no:5, October November 2015, 1916-1920.

[18] VF Korshak I.V Postavnichii, NV Tkchenko, Changes in the heat of melting of a super elastic eutectic Sn30 wt% Pb alloy due to preliminary plastic deformation, The Physics of metal and metallography, vol no: 116 issue no: 10, 2015, 1029-1034.

[19] Adnan I O Zaid, Moham mad M Al-Tamimi, Cavity closure during compression between semi-closed dies using superplastic tin-lead alloy, Materials Science and Engineering, 2013 1-8.

[20] Erick Petta Marinho, Alberto Sakata, Erika Fernanda Prados, Gilmar Ferreira Batalha, Instrumentation and Control of a Bulge Test on a Superplastic Pb-Sn Alloy, Superplasticity in Advanced Materials ICSAM 2012 Vol no: 735 2013 224-231.

[21] Kawasaki Vitor Luiz Sordi Megumi, Achieving superplastic properties in a Pb–Sn eutectic alloy processed by equal-channel angular pressing, Journal of Materials Science vol no :46 ,issue no:1, January 2011, 155160.

[22] J.J.V Jayasing, B Nageshwar rao, Gas pressure forming of spherical domes from lead tin eutectic alloy superplastic sheet material, Materials Science vol no:2 issue no:3 2008 241-258.

[23] Robert braga figueiredo, Paulo maria, Micro structure and mechanical properties of Pb-4%Sb alloy processed by equal channel angular pressing, Materials research vol no:9, issue no:1,2006 101-106.

[24] K. Kalaichelvan S. Venkatasamy, Experimental analysis of macro-micro superplastic forming on pb-sn eutectic alloy sheets, Institution of engineers india part mm metallurgy and material science division vol no:85 April 2004 13-17.

[25] Megumi Kawasakia, Sangmok Leea, Terence G. Langdona, Constructing a deformation mechanism map for a superplastic Pb–Sn alloy processed by equal-channel angular pressing, Scripta Materialia, vol no:61 issue no:10 November 2009 963-966.

[26] A Huang, A Lowe, M.J Cardew-Hall, Experimental validation of sheet thickness optimization for superplastic forming of engineering structures materials Processing Technology vol no:113 issue no:1 3 May 2001 136-143.

[27] F.S. Qu, Z. Lu, F. Xing, K.F. Zhang, Study on laser beam welding/superplastic forming technology of multi-sheet cylinder sandwich structure for Inconel718 superalloy with ultra-fine grains, Materials and Design 39 (2012) 151–161.

[28] Jun Liu, Ming-Jen Tan, Anders E W Jarfors, Samuel C V Lim, Kai-Soon Fong, Sylvie Castagne, Greener manufacturing: Superplastic-like forming, ECO-MATES2011 IOP Publishing, Journal of Physics: Conference Series 379 (2012) 012034.

[29] Zhang Datong, Chai Fang, Li Yuanyuan, High strain rate superplasticity of a fine-grained AZ91Magnesium alloy prepared by friction stir processing, The 8th Pacific Rim International Congress on Advanced Materials and Processing, pp. 1065 – 1072.

[30] Adnan I O Zaid, Mohammad M Al-Tamimi, Cavity closure during compression between semi-closed dies using superplastic tin-lead alloy, International Symposium on Advanced Materials (ISAM 2013).

[31] B. P. Kashyap, Overview: Experimental Constitutive Relationship for High Temperature Deformation and the Effect of Concurrent.

[32] Microstructure Evolution, Indian Institute of Metals, DOI 10.1007/s12666-015-0751-1.

[33] G. Kumaresan and A. Jothilingam, Experimental and FE simulation validation of sheet thickness optimization in superplastic forming of Al alloy, Journal of Mechanical Science and Technology 30 (7) (2016) 3295~3300.

[34] A. Kishchik, A. V. Mikhaylovskaya, V. S. Levchenko, V. K. Portnoy, Formation of Microstructure and the Superplasticity of Al–Mg-Based Alloys, ISSN 0031-918X, Physics of Metals and Metallography, 2017, Vol. 118, No. 1, pp. 96–103. Pleiades Publishing, Ltd., 2017